J Fluoresc (2009) 19:837–845
DOI 10.1007/s10895-009-0481-z

ORIGINAL PAPER

Fluorescence Spectroscopic Properties Analysed within the Extended Förster Theory with Application to Biomacromolecular Systems

N. Norlin · P.-O. Westlund · L. B.-Å. Johansson

Received: 27 February 2009 / Accepted: 27 March 2009 / Published online: 5 May 2009

Abstract The extended Förster theory (EFT) of electronic energy transport accounts for translational and rotational dynamics, which are neglected by the classical Förster theory (FT). EFT has been developed for electronic energy transfer within donor-acceptor pairs [Isaksson, *et al*, *Phys. Chem. Chem. Phys.*, **9**, 1941(2007)] and donor-donor pairs [Johansson, *et al*, *J. Chem. Phys.*, **105**, 10896 (1996); Norlin, *et al*, *Phys. Chem. Chem. Phys.*, **10**, 6962(2008)]. For donors that exhibit different or identical *non-exponential* fluorescence relaxation within a donor-donor pair, the process of reverberating energy migration is reversible to a higher or lower degree. Here the impact of the EFT has been studied with respect to its influence on fluorescence quantum yields, fluorescence lifetimes as well as depolarisation experiments. The FT predicts relative fluorescence quantum yields which usually agree with the EFT within experimental accuracy, however, substantial deviations occurs in the steady-state and in particular the time-resolved depolarisation data.

Keywords Electronic energy migration · Homotransfer · Donor-Donor Energy Migration (DDEM) · Partial Donor-Donor Energy Migration (PDDEM)

Abbreviations

A	acceptor of electronic energy
D_j	the j-th donor
$\mathbf{D}_j$	director frame for the j-th donor
DDEM	donor-donor energy migration
EFT	extended Förster theory
EM	energy migration
FT	Förster theory
F(t)	fluorescence decay
κ	the angular dependence of dipole-dipole coupling
$\langle\kappa^2\rangle$	the mean-squared angular part of dipole-dipole coupling in the fast dynamic limit
L	laboratory frame
$\Lambda = (R_0/R)^6$	the coupling strength
M_j	molecule fixed frame for the j-th donor
PDDEM	partial donor-donor energy migration
R	the distance between the centres of mass of the donor groups
R_0	the Förster radius
$\mathbf{R}$	coordinate system fixed in a macromolecule
S_j	2^{nd} rank order parameter of the j-th donor
τ_J	the fluorescence lifetime of the donor J
ϕ_J	the rotational correlation time of donor J
ω	the rate of energy migration
Ω_{D_jR}	short-hand notation for the configuration angles

N. Norlin · P.-O. Westlund · L. B.-Å. Johansson (✉)
Department of Chemistry; Biophysical Chemistry,
Umeå University,
Umeå S-901 87, Sweden
e-mail: lennart.johansson@chem.umu.se

Introduction

Following the pioneering paper about "the chemical ruler"[1] by Haugland and Stryer, several studies have dealt with the estimation of inter- and intramolecular distances in biomacromolecular structures[2–4]. The classical Förster theory (FT)[5], however completely neglects the influence of distance fluctuations and rotational dynamics of the interacting chromophores, as well as the fact the

energy transfer/migration occurs in locally anisotropic systems. In most applications the influence of translational dynamics can be neglected, whereas usually not the influence of rotational dynamics and local anisotropy. The latter question is often referred to as "the κ^2-problem", which has been studied by several scientists [6–9]. This problem has been overcome by reconsidering the derivation of the FT. The extended Förster theory (EFT) then obtained is a stochastic master equation which is derived from the stochastic Liouville equation of motion [10–13]. In fact, the EFT accounts for the reorientational, as well as the translational motions of the interacting chromophores.

Quite often fluorescence spectroscopic studies are performed on proteins, which contain two or more intrinsic (*e.g.* tryptophan, flavins), or extrinsic fluorescent groups (*e.g.* rhodamines, fluorescein, ANS). Electronic energy is then transported among these chemically identical groups. The fluorescence decay of each group is usually not the same in absence of the other groups. An important example is Trp, which has been thoroughly studied[4, 14, 15], as well as several of the most commonly used fluorescent probes[4]. Therefore, the observed fluorescence decay of two interacting fluorophores is not given by the arithmetic average of the fluorescence decay of each fluorophore in the absence of electronic energy transport. This holds even if the back and forward rates of energy migration are equal, as would be expected for two differently localised fluorophores which exhibit the same overlap between the absorption and fluorescence spectra. The BODIPY fluorophore is a nice example of the latter case[16]. The ultimate conditions for a pure donor-donor energy migration would be two donor groups which exhibit equal single exponential fluorescence decays and spectral overlaps. As a consequence, the photophysics decay becomes invariant to the donor-donor energy migration (DDEM) process, which is also referred to as homotransfer[2]. However, this is not strictly true for donors exhibiting a *non*-exponential fluorescence. This situation resembles something in between DDEM and donor-acceptor energy transfer, which previously has been referred to as partial donor-donor energy migration (PDDEM)[17]. Recently, the EFT for PDDEM was derived[13], which justifies asking: What is the influence of the EFT on commonly studied spectroscopic properties like the fluorescence quantum yield, the fluorescence relaxation, the steady-state and the time-resolved fluorescence depolarisation/ anisotropy? In the EFT the interesting spectroscopic properties are obtained by solving stochastic equations, which make it difficult to *a priori* predict the result. The theoretical expressions become less transparent and also the application of the theory challenging. In order to picture for instance, the fluorescence depolarisation or the fluorescence relaxation, Brownian dynamics simulations are needed to accurately describe the stochastic reorientation of the fluorescent molecules. Thus, basically a numerical testing procedure is needed. A critical reader might therefore ask; why and to what extent this theoretical approach is preferable prior the FT? The former question is easy to answer and has already been pointed out[11, 13]. In most studies that include energy transfer/migration processes, the influence of molecular rotational motions and anisotropic rotational restrictions are not negligible. The answer to the latter question is the main motivation for the present paper. Since myriads of possible experimental circumstances are possible, it is necessary to select the conditions for which approximations of the EFT are most difficult to achieve. This occurs when the rates of energy transport and reorientations are similar. More precisely, for values of the Kubo numbers (ϑ) which are beyond the perturbation regime, *i.e.* $\vartheta \geq 1$[18]. On this basis, the molecular properties of the donor-donor systems studied here, have carefully been selected. These form a basis for generating data, which mimics different fluorescence spectroscopic experiments. This also enables to examine the pronounced discrepancies between the EFT and the classical Förster theory.

Computational methods

The time-resolved fluorescence lifetime decay and depolarisation, as well as the relative fluorescence quantum yield steady-state fluorescence anisotropy have been calculated using the EFT for the case of partial donor-donor energy migration. BD simulations have been used to model the molecular reorientation of fluorophores attached to a slowly tumbling and rigid macromolecule. The method has previously been extensively described[19] and later applied for analyses of time-correlated single-photon counting experiments[20, 21]. Throughout this work a cone potential describes an assumed local anisotropy in the BD simulations. A unit vector representing the transition dipole moment of the donor or the acceptor group undergoes restricted diffusion on a sphere, while it is forced to exist within the confines of the cone potential.

The time-resolved fluorescence decays were simulated for a duration of 50 ns, which was divided into 1000 intervals of time. The photophysics of each fluorophore was assumed to be a bi-exponential function with equal pre-exponential factors of the lifetime components 1 and 5 ns. The reorientation correlation times (ϕ) of each donor were chosen according to the criteria specified as the cases I-IV in Table 1. Furthermore, the condition $\phi = \Lambda^{-1}\langle\kappa^2\rangle^{-1}$ was fulfilled for the isotropic as well as the anisotropic cases.

The numerical procedures start by generating stochastic trajectories of a reorienting transition dipole. From these

Table 1 Considered properties of bifluorophoric macromolecules isotropically distributed in a liquid solution. The local orientation of the interacting fluorophores (j = α and β) are either random (R) or uniaxially anisotropic (U). Each fluorophore exhibits the same bi-exponential fluorescence decay (*cf.* Eq. 1). For all anisotropic systems the local molecular order parameter was assumed to be $S = \left\langle D_{00}^{(2)}(\beta_{M_jD_j})\right\rangle = 0.745$. The configuration angles $\Omega = (\alpha_D, \beta_{D_\alpha R}, \beta_{D_\beta R})$ describe the orientation of the anisotropic distribution with respect to a coordinate frame that connects the centres of mass of the two chromophores. The value of the square-mean orientation value of dipole-dipole coupling ($\langle\kappa^2(\Omega)\rangle$) refers to the fast dynamic limit [6]

Case	Ω	$\langle\kappa^2(\Omega)\rangle$	Rotational Correlation Times
R1	ND = 0	2/3	$\phi_\alpha = \phi_\beta = \tau_{\alpha1} = \tau_{\beta1}$= 1 ns
R2	ND = 0	2/3	$\phi_\alpha = \phi_\beta = \tau_{\alpha2} = \tau_{\beta2}$= 5 ns
R3	ND = 0	2/3	$\phi_\alpha = \phi_\beta = (\tau_{\alpha1} + \tau_{\alpha2})/2$= 3 ns
R4	ND = 0	2/3	$\phi_\alpha = \tau_{\alpha1} = 1\,ns \quad \phi_\beta = \infty$
R5	ND = 0	2/3	$\phi_\alpha = \tau_{\alpha2} = 5\,ns \quad \phi_\beta = \infty$
U1	(45°, 58°, 29°) = I	0.35	$\phi_\alpha = \phi_\beta = \tau_{\alpha1} = \tau_{\beta1}$= 1 ns
U2	(45°, 58°, 29°) = I	0.35	$\phi_\alpha = \phi_\beta = \tau_{\alpha2} = \tau_{\beta2}$= 5 ns
U3	(45°, 58°, 29°) = I	0.35	$\phi_\alpha = \phi_\beta = (\tau_{\alpha1} + \tau_{\alpha2})/2$= 3 ns
U4	(45°, 58°, 29°) = I	0.35	$\phi_\alpha = \tau_{\alpha1} = 1\,ns \quad \phi_\beta = \infty$
U5	(45°, 58°, 29°) = I	0.35	$\phi_\alpha = \tau_{\alpha2} = 5\,ns \quad \phi_\beta = \infty$
U1	(40°, 40°, 11°) = II	0.72	$\phi_\alpha = \phi_\beta = \tau_{\alpha1} = \tau_{\beta1}$= 1 ns
U2	(40°, 40°, 11°) = II	0.72	$\phi_\alpha = \phi_\beta = \tau_{\alpha2} = \tau_{\beta2}$= 5 ns
U3	(40°, 40°, 11°) = II	0.72	$\phi_\alpha = \phi_\beta = (\tau_{\alpha1} + \tau_{\alpha2})/2$= 3 ns
U4	(40°, 40°, 11°) = II	0.72	$\phi_\alpha = \tau_{\alpha1} = 1\,ns \quad \phi_\beta = \infty$
U5	(40°, 40°, 11°) = II	0.72	$\phi_\alpha = \tau_{\alpha2} = 5\,ns \quad \phi_\beta = \infty$
U1	(41°, 12°, 71°) = III	1.60	$\phi_\alpha = \phi_\beta = \tau_{\alpha1} = \tau_{\beta1}$= 1ns
U2	(41°, 12°,71°) = III	1.60	$\phi_\alpha = \phi_\beta = \tau_{\alpha2} = \tau_{\beta2}$= 5 ns
U3	(41°, 12°,71°) = III	1.60	$\phi_\alpha = \phi_\beta = (\tau_{\alpha1} + \tau_{\alpha2})/2$= 3 ns
U4	(41°, 12°,71°) = III	1.60	$\phi_\alpha = \tau_{\alpha1} = 1\,ns \quad \phi_\beta = \infty$
U5	(41°, 12°,71°) = III	1.60	$\phi_\alpha = \tau_{\alpha2} = 5\,ns \quad \phi_\beta = \infty$

the stochastic rates of energy transport as well as the reorientation correlation functions were calculated. Each pairwise combination of lifetimes contributes to the total excitation probability and the anisotropy. A detailed outline of the theory is presented elsewhere[10, 13]. The fluorescence decay curves, $F_{||}$(t) and $F_{\perp}$(t), were generated in accordance with Eq. 9 (*cf.* Theoretical Prerequisites). The simulated data were averaged over at least 10^6 trajectories. In the calculation of the Kubo number and the κ^2-reorientational correlation functions 10^7 trajectories were used.

The steady-state intensities $F_{||}$ and $F_{\perp}$ were obtained from a time-integration of $F_{||}$(t) and $F_{\perp}$(t) and these values were then used for calculating the steady-state anisotropy. The relative quantum yield of fluorescence was defined by the ratio between the integrated photophysics decay and the integrated photophysics in the absence of coupling. All computer programs were written in C and the calculations were performed using a Suse 9.2 Linux cluster.

Theoretical prerequisites

In the following, electronic energy transport is studied within two chemically and photophysically identical fluorophores, schematically illustrated in Fig. 1. Both fluorophores D_α and D_β exhibit an identical fluorescence decay, which is described by a sum of two exponential functions according to:

$$F_i(t) = \sum_{j=1}^{2} a_{ij} \exp(-t/\tau_{ij}) \qquad i = \alpha, \beta \tag{1}$$

The bi-exponentiality could be ascribed to the presence of two photophysically different forms of the fluorophore. Here primarily the case for which $a_{\alpha j} = a_{\beta j} = 1/2$ and $\tau_{\alpha j} = \tau_{\beta j}$ has

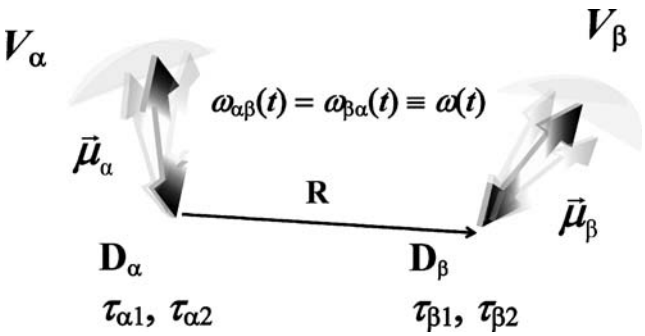

Fig. 1 Schematic of two interacting electronic transition dipoles ($\vec{\mu}$) of the chemically identical chromophores D_α and D_β, where each donor D_j exhibits a bi-exponential fluorescence relaxation according to Eq. 1. The donors undergo local reorienting motions with respect to the frames $\mathbf{D}_\alpha$ and $\mathbf{D}_\beta$ which are interconnected at a fixed distance (R) by the macromolecular frame (**R**). The anisotropic orienting potentials are denoted V_α and V_β

been considered. As a consequence, the energy migration in such a system constitutes DDEM and PDDEM between the fluorophores having equal and different fluorescent lifetimes, respectively.

Moreover, it is assumed that the donors undergo reorienting motions in the potentials (V_i) and that these are located at a mutual distance R (*cf.* Fig. 1). In the simplest case considered, both donors are assumed to undergo isotropic reorientation. A uniaxial anisotropic potential was approximated by cone potential with a cone angle of 35°. Using this potential one obtains the second rank order parameter values of $S_\alpha = S_\beta = \left\langle D^{(2)}_{0,0}(\Omega_{M_iD_i})\right\rangle = 0.745$. The uniaxial symmetry defines a director frame, with respect to a common **R**-frame (*cf.* Fig. 1). These orientation angles are denoted Ω_{D_iR}, hereafter referred to as the *configuration angles*. Three different sets of configuration angles, *i.e.* three *configurations*, have been examined (*cf.* Table 1). In the following, the relevant equations for describing the influence of DDEM and PDDEM on various experimental fluorescence spectroscopic properties are presented.

Fluorescence quantum yield

The system investigated is composed of an ensemble of $D_\alpha D_\beta$ pairs which are randomly distributed, as in a liquid solution. Each pair is specifically bonded to a macromolecule that undergoes a negligible reorientation on the timescale of fluorescence. Previously, the excitation probability [$\chi_i(t)$] has been derived from the EFT. The probabilities obtained for the primarily (p) and the secondary (s) donor groups and in the case of DDEM are given in reference[10]. In the theory the excitations probabilities are defined within a pair with the lifetimes $\tau_{\alpha j} = \tau_{\beta j} = \tau$. However, two pairs are considered which below are indicated by the index j:

$$\begin{aligned}\chi^{p}_{ij}(t) &= \widetilde{\chi}^{p}_{ij}(t)\exp(-t/\tau_{ij}) \\ &= \left\{1-\widetilde{\chi}^{s}_{ij}(t)\right\}\exp(-t/\tau_{ij}) \quad i\in\alpha,\beta \text{ and } j=1,2 \\ \widetilde{\chi}^{p}_{ij}(t) &= \left\langle 1+\exp(-\int_0^t 2\omega(t')dt')\right\rangle/2\end{aligned} \tag{2}$$

In Eq. 2 the bracket ($\langle ... \rangle$) denotes an average over the rate of energy migration, $\omega(t)=\kappa^2(t)\Lambda$, where $\kappa^2(t)$ and $\Lambda\left\{=(R_0/R)^6\right\}$ denote the angular part and the strength of dipole-dipole coupling, respectively. The corresponding excitation probabilities for PDDEM [*i.e.* $\chi^{p}_{ijk}(t)$, $\chi^{s}_{ijk}(t)$, where i = α,β , while j ≠ k = 1,2 refers to the numbering of the lifetime components] are obtained by numerically solving the stochastic master equation[13].

Since the fluorescence relaxation is invariant to the DDEM process (*cf.* Eq. 2) only the PDDEM contributes to the time-resolved fluorescence decay ($F_{\alpha\beta}(t)$) and the steady-state intensity ($F_{\alpha\beta}$). The relative quantum yield of fluorescence is then given by:

$$\begin{aligned}\Phi_{Fr} &= \frac{F_{\alpha\beta}}{\int_0^\infty (F_\alpha(t)+F_\beta(t))dt} \\ &= \frac{\sum_{i=\alpha,\beta}\left[\sum_{j=1}^{2}\tau_{ij}+\sum_{j\neq k=1}^{2}\int_0^\infty\left\langle\left(\chi^{s}_{ijk}(t)+\chi^{p}_{ijk}(t)\right)\right\rangle dt\right]}{2\sum_{i=\alpha,\beta}\sum_{j=1}^{2}\tau_{ij}}\end{aligned} \tag{3}$$

The quantum yield was also calculated in the FT approximation. For this, the excitation probabilities ($\chi^{p}_{ijk}(t)$, $\chi^{s}_{ijk}(t)$) are given by analytical expressions, which are solutions of the master equation of PDDEM[17].

It is assumed that the measured fluorescence intensity has been collected under the "magic angle" condition[4]. Note that in Eq. 3, as well as in the following equations it is assumed that $a_{\alpha j} = a_{\beta j} = 1/2$ (*cf.* Eq. 1).

Fluorescence depolarisation experiments

Time-resolved fluorescence depolarisation data are used to construct the time-resolved fluorescence anisotropy[4, 22]. This anisotropy is an orientation correlation function of second rank, which depends on the reorienting motions of an excited fluorescent molecule, as well as the energy migration process. Furthermore, the rate of energy transport also depends on the rate of reorientation. For an ensemble of non-interacting donor molecules exhibiting identical photophysics the fluorescence anisotropy is given by

$$r(t) = r_0\langle P_2[\widehat{\mu}(0)\cdot\widehat{\mu}(t)]\rangle \equiv r_0\rho(t) \tag{4}$$

In Eq. 4, r_0, $\langle ..... \rangle$, and P_2 denote the fundamental anisotropy[23], the ensemble orientational average and the second Legendre polynomial, respectively. The orientation of the electronic transition dipole moment at the times of excitation ($t = 0$) and emission ($t = t$) are denoted by the unit vectors $\widehat{\mu}(0)$ and $\widehat{\mu}(t)$. For the D_α and D_β groups, the correlation functions of an initially excited donor, which is emitting a photon are denoted $\rho_{\alpha\alpha}(t)$and $\rho_{\beta\beta}(t)$, respectively. An additional contribution to the fluorescence depolarisation originates from the emission from a donor, say β, which has been excited via energy migration from the initially excited α-donor, or *vice versa*. These contributions are $\rho_{\beta\alpha}(t)(=P_2\left[\widehat{\mu}_\beta(0)\cdot\widehat{\mu}_\alpha(t)\right])$ and $\rho_{\alpha\beta}(t)(=P_2[\widehat{\mu}_\alpha(0)\cdot\widehat{\mu}_\beta(t)])$, respectively. The weight of the different correlation functions is determined by the actual excitation probability

of the described scenarios. Thus the obtained anisotropy can be written,

$$r(t) = r_0 \frac{\left\langle \sum\limits_{i=\alpha,\beta} \rho_{ii}(t) \sum\limits_{j\neq n=1}^{2} \left(\widetilde{\chi}^{p}_{ij}(t)\exp(-t/\tau_{ij}) + \chi^{p}_{ijn}(t) \right) \right\rangle + \left\langle \sum\limits_{i\neq k=\alpha,\beta} \rho_{ik}(t) \sum\limits_{j\neq n=1}^{2} \left(\widetilde{\chi}^{s}_{kj}(t)\exp(-t/\tau_{kj}) + \chi^{s}_{kjn}(t) \right) \right\rangle}{\sum\limits_{i=\alpha,\beta} \left(\sum\limits_{j=1}^{2} \exp(-t/\tau_{ij}) + \sum\limits_{j\neq n=1}^{2} \left\langle \chi^{p}_{ijn}(t) + \chi^{s}_{ijn}(t) \right\rangle \right)} \tag{5}$$

One should note that the fluorescence anisotropy decay is not invariant to the energy migration process, whereas it would be for very similar lifetimes, *i.e.* $\tau_{ij} \rightarrow \tau$, whereby $\chi^{p}_{ijn}(t) \rightarrow \widetilde{\chi}^{p}_{ij}(t)\exp(-t/\tau)$ and $\chi^{s}_{kjn}(t) \rightarrow \widetilde{\chi}^{s}_{kj}(t)\exp(-t/\tau)$. Within this approximation Eq. 5 can be rewritten as:

$$r(t) = \frac{r_0}{2} \left\langle \sum_{i=\alpha,\beta} \sum_{j=1}^{2} \rho_{ii}(t) \widetilde{\chi}^{p}_{ij}(t) + \sum_{i\neq k=\alpha,\beta} \sum_{j=1}^{2} \rho_{ik}(t) \widetilde{\chi}^{s}_{kj}(t) \right\rangle \tag{6}$$

A detailed description of the different angular transformations, which are needed to evaluate the orientation functions $\rho_{ij}(t)$ are given elsewhere[13]. In brief, the molecular electronic transition dipole moment is considered to be distributed in a uniaxially symmetric manner with respect to a rigidly attached coordinate system in the macromolecule. To mimic a liquid solution this director frame is isotropically oriented with respect to the laboratory frame. The reorientation correlation function for each donor is conveniently in terms of Wigner rotation matrix elements[24];

$$\rho_{ii}(t) = \sum_{m=-2}^{2} \left\langle D^{(2)}_{m,0}(\Omega^{0}_{M_iD_i}) D^{(2)}_{-m,0}(\Omega_{M_iD_i}, t) \right\rangle (-1)^{m} \tag{7}$$

while for the coupled donors. $i \neq j$, one obtains:

$$\rho_{ij}(t) = \sum_{q,q',m} D^{(2)}_{m,q}(\Omega_{D_iR}) D^{(2)}_{-m,q'}(\Omega_{D_jR}) \left\langle D^{(2)}_{q,0}(\Omega^{0}_{M_iD_i}) D^{(2)}_{q',0}(\Omega_{M_jD_j}, t) \right\rangle (-1)^{m} \tag{8}$$

The Euler angles that transform the transition dipole to a fixed and immobilised director frame at the times $t = 0$ and $t = t$ are denoted $\Omega^{0}_{M_iD_i}$ and $\Omega_{M_iD_i}$, respectively. The orientations of the two director frames relative to a common **R**-frame are defined by the configuration angles Ω_{D_iR}.

Steady-state fluorescence depolarisation data can be obtained from the fluorescence intensity decays of $F_{\|}(t)$ and $F_{\perp}(t)$. Experimentally the obtained steady-state intensities, $F_{\|}$ and $F_{\perp}$ are collected with the emission polariser set parallel (||) and perpendicular ($\perp$) relative to the excitation polariser[4]. In terms of contribution from the different correlation functions $[\rho_{ij}(t)]$ and excitation probabilities $[\chi^{n}_{m}(t)]$ these observables are given by;

$$\begin{aligned} F_{||}(t) &= C\left\{ \sum_{i=\alpha,\beta} \sum_{j\neq n=1}^{2} \left\langle (1 + 2r_0\rho_{ii}(t)) \left(\widetilde{\chi}^{p}_{ij}(t)\exp(-t/\tau_{ij}) + \chi^{p}_{ijn}(t) \right) \right\rangle + \sum_{i\neq k=\alpha,\beta} \sum_{j\neq n=1}^{2} \left\langle (1 + 2r_0\rho_{ik}(t)) \left(\widetilde{\chi}^{s}_{kj}(t)\exp(-t/\tau_{kj}) + \chi^{s}_{kjn}(t) \right) \right\rangle \right\} \\ F_{\perp}(t) &= C\left\{ \sum_{i=\alpha,\beta} \sum_{j\neq n=1}^{2} \left\langle (1 - r_0\rho_{ii}(t)) \left(\widetilde{\chi}^{p}_{ij}(t)\exp(-t/\tau_{ij}) + \chi^{p}_{ijn}(t) \right) \right\rangle + \sum_{i\neq k=\alpha,\beta} \sum_{j\neq n=1}^{2} \left\langle (1 - r_0\rho_{ik}(t)) \left(\widetilde{\chi}^{s}_{kj}(t)\exp(-t/\tau_{kj}) + \chi^{s}_{kjn}(t) \right) \right\rangle \right\} \end{aligned} \tag{9}$$

From a time-integration of the intensities given by Eq. 9, one obtains the steady-state intensities $\left(F_{\|}, F_{\perp}\right)$, which enable calculations of the fluorescence steady-state anisotropy (r) according to the well known definition: $r \equiv \left(F_{\|} - F_{\perp}\right)/\left(F_{\|} + 2F_{\perp}\right)$.

Systems studied and implications thereof

The aim is to examine the influence of electronic energy transport and reorientational dynamics within pairs of chemically and photophysically identical chromophores.

Each donor exhibits equal, but a *non*-exponential fluorescence decay. For the sake of simplicity, it is then assumed that the fluorescence decay of each donor (α or β) exhibits the same bi-exponential fluorescence decay in the absence of Förster coupling (*cf.* Eq. 1). In the presence of energy transport, DDEM occurs between the species of equal lifetime (*i.e.* $\tau_{\alpha i} = \tau_{\beta i}$), whereas PDDEM occurs between the species of different lifetimes. The intension here is to demonstrate the influence of this complexity on various commonly studied fluorescence spectroscopic properties. These refer to the fluorescence quantum yield, time-resolved fluorescence relaxation, as well as the fluorescence steady-state and time-resolved anisotropy. The previous section outlines the relations between these spectroscopic properties and the extended Förster theory of DDEM, as well as PDDEM. In numerous published applications of the FT, the interaction is assumed to occur in the fast dynamic limit and among *isotropically* or *randomly* oriented chromophores, for which $\langle \kappa^2 \rangle = 2/3$[6]. The fast dynamic limit means that the reorienting rates are much faster than the rates of energy transport. This value of $\langle \kappa^2 \rangle$ is frequently used even for chromophoric groups localised in, *e.g.* a protein or a DNA structure, where the assumption is rarely true. Typically the local reorienting motions of covalently protein-linked fluorescent groups are comparable to the fluorescence lifetimes. Furthermore, it would be appropriate to consider an anisotropic order, while an isotropic approximation could only be justified for very flexible chromophores, *i.e.* for a local order that could be approximated by low values of the order parameter. One should note that information about the local order can be obtained from fluorescence depolarisation studies of each fluorophore in the absence of coupling[8]. In this work the isotropic approximation, as well as examples of locally anisotropic order have been extensively examined. Also examined is the influence of reorientation dynamics for rotational correlation times which either are short, intermediate, equal, or infinite (*i.e.* the static case for one of the donors) as compared to the longest lifetime component (= 5 ns). Most of the studied systems are defined in Table 1.

Relative fluorescence quantum yield and relaxation

The relative fluorescence quantum yields have been calculated for different configurations and strengths of coupling (*cf.* Tables 2 and 3). In these calculations the true value as obtained within the EFT are compared with the values predicted by using the common approach of the Förster theory. Since one deals with DDEM, or homotransfer, it generally would be assumed that the relative quantum yield is unity. However, this is not true as shown by the calculated data, which are displayed in the Tables 2 and 3. The general pattern shows that the values obtained in the EFT and FT-approximation are rather similar. Since the typical errors in quantum yield determinations are 5 – 10 % the approximate value obtained by FT is usually experimentally indistinguishable from the EFT result. The time-resolved fluorescence decays displayed in Fig. 2 typically

Table 2 The relative fluorescence quantum yield (Φ_{Fr}) and the steady-state anisotropy (r) calculated by using Eq. 3 for different cases (1-5) and configurations (Ω = 0, I-III) of DDEM and PDDEM within $D_\alpha D_\beta$ pairs. The relative quantum yield is defined by the ratio of the fluorescence quantum yields obtained in the presence and the absence of energy transport. The local orientations of the interacting fluorophores D_α and D_β are either randomly oriented (R) or uniaxially anisotropic (U). The expected values of the steady-state anisotropies in the absence of EM processes (r^0), as well as within the Förster theory (r_{FT}) are also displayed, when assuming the isotropic dynamic value of $\langle \kappa^2 \rangle = 2/3$

Case & Ω (= 0, I-III)	Λ	Φ_{Fr} **(EFT)**	Φ_{Fr} **(FT)**	r	r_{FT}	r^0
R10	1.500	0.824	0.811	0.078	0.074	0.084
R20	0.300	0.897	0.880	0.187	0.181	0.206
R30	0.500	0.871	0.854	0.148	0.142	0.162
R40	1.500	0.829	0.811	0.167	0.155	0.242
R50	0.300	0.901	0.880	0.253	0.240	0.303
U1I	2.890	0.828	0.797	0.237	0.226	0.262
U2I	0.578	0.902	0.847	0.299	0.280	0.319
U3I	0.963	0.877	0.825	0.277	0.260	0.299
U4I	2.890	0.837	0.797	0.279	0.259	0.331
U5I	0.578	0.907	0.847	0.328	0.300	0.360
U1II	1.390	0.831	0.814	0.257	0.256	0.262
U2II	0.278	0.903	0.885	0.309	0.307	0.319
U3II	0.463	0.878	0.857	0.291	0.288	0.299
U4II	1.390	0.839	0.814	0.297	0.291	0.331
U5II	0.278	0.907	0.885	0.337	0.331	0.360
U1III	0.626	0.818	0.843	0.208	0.218	0.262
U2III	0.125	0.889	0.927	0.280	0.293	0.319
U3III	0.209	0.863	0.900	0.254	0.267	0.299
U4III	0.626	0.820	0.843	0.245	0.257	0.331
U5III	0.125	0.892	0.927	0.308	0.323	0.360

Table 3 The relative fluorescence quantum yield (Φ_{Fr}) and the steady-state anisotropy (r) calculated by using Eq. 3 for DDEM and PDDEM within $D_\alpha D_\beta$ pairs with the strengths of different strengths coupling (Λ) and the configurations, Ω = III, IV. The configuration IV corresponds to Ω = (89°, 89°, 89°), whereas the configuration III is defined in Table 1. The relative quantum yield is defined by the ratio of the fluorescence quantum yields obtained in the presence and the absence of energy transport. The local orientations of the interacting fluorophores are uniaxially anisotropic (U). The obtained values of the steady-state anisotropies for $\Lambda = 0$ means that only the reorienting dynamics contribute. The anisotropy predicted by the FT (r_{FT}) assume that the isotropic dynamic value of $\langle\kappa^2\rangle = 2/3$

Case & Ω	Λ	Φ_{Fr} (EFT)	Φ_{Fr} (FT)	r	r_{FT}
U2III	0	1.000	1.000	0.319	0.319
U2III	1.25 10^{-3}	0.997	0.999	0.318	0.319
U2III	4.13 10^{-2}	0.941	0.969	0.300	0.309
U2III	0.125	0.889	0.927	0.280	0.293
U2III	0.213	0.861	0.896	0.267	0.281
U2III	0.413	0.836	0.862	0.253	0.266
U2III	2.41	0.796	0.801	0.227	0.230
U2IV	0	1.000	1.000	0.319	0.319
U2IV	1.25 10^{-3}	0.999	0.999	0.319	0.319
U2IV	4.13 10^{-2}	0.991	0.969	0.313	0.295
U2IV	0.125	0.976	0.927	0.302	0.261
U2IV	0.213	0.963	0.899	0.292	0.239
U2IV	0.413	0.940	0.862	0.275	0.206
U2IV	2.41	0.866	0.801	0.214	0.141
U2IV	12.4	0.816	0.784	0.161	0.120

illustrate the small differences between the photophysics relaxation of the EFT and the FT decays.

Fluorescence anisotropy

The steady-state fluorescence anisotropies obtained for different configurations and strengths of coupling have been calculated. The obtained results are summarised in the Tables 2 and 3. The data compares the true value obtained within the EFT, with the values predicted by using the common approach of the Förster theory. The typical accuracy of modern spectrometers makes it possible to determine steady-state values within ± 0.005, at least for fluorophores exhibiting moderate to high yields of fluorescence. In general, the steady-state values predicted by the EFT are somewhat higher than those obtained within the FT for rotational correlation times, $\phi_c = \Lambda^{-1}\langle\kappa^2\rangle^{-1}$. For an almost perpendicular configuration (*cf.* Ω = IV in Table 3) the deviations between are substantial and often large enough to be experimentally distinguishable. The influence of Λ on the steady-state anisotropy and Φ_{Fr} has also been studied. For the two configurations examined, the discrepancy between the values predicted by the EFT and the FT increases with increasing Λ and reaches a maximum deviation for Kubo numbers of about unity.

Taken together, the steady-state anisotropy and Φ_{Fr} data obtained with the EFT and the FT and displayed in Tables 2 appears very similar, but evidently there is a dependence on the coupling strength, as shown in Table 3. This demonstrates the importance of accounting for the dynamics and the local order. To examine the impact of these properties, it is interesting to compare the time-resolved fluorescence anisotropy predicted by the extended and the conventional description of energy transfer. The time-resolved depolarisation data predicted for the configurations Ω = UI – UIII and the cases 1–5 are presented in Fig. 3. It is evident that the decay curves corresponding to the FT and the EFT can exhibit different relaxation rates, as well as stationary levels of the anisotropy, *i.e.* the infinity values denoted $r(t_\infty)$. Therefore it would not be surprising if both theories predict very similar values on the integrated time-resolved anisotropy. For instance, consider the data shown in Fig. 3 for case 5. Here, the integrated values of $r_{EFT}(t)$ and $r_{FT}(t)$ often happens to be very similar, and consequently also the corresponding steady-state values (*cf.* Table 2).

In the limit of very fast energy migration and reorientations the time-dependence of the fluorescence anisotropy reaches a stationary value for which the orientation correlation between initially excited and emitting donors vanishes. In this limit the plateau value is given by:

$$r(t_\infty) = r_0 \left\{ \begin{array}{l} \left\langle D_{00}^{(2)}(\beta_{M_\alpha D_\alpha})\right\rangle^2 + \left\langle D_{00}^{(2)}(\beta_{M_\beta D_\beta})\right\rangle^2 \\ + \left\langle D_{00}^{(2)}(\beta_{M_\alpha D_\alpha})\right\rangle \left\langle D_{00}^{(2)}(\beta_{M_\beta D_\beta})\right\rangle D_{00}^{(2)}(\delta) \end{array} \right\}, \tag{10}$$

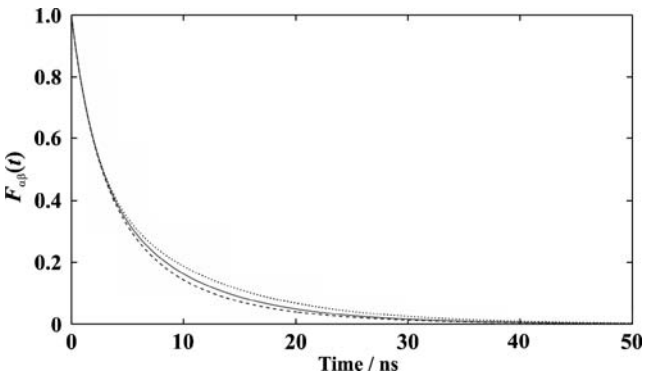

Fig. 2 The photophysics predicted by the EFT, in the absence (*dotted line*) and the presence (*solid line*) of energy migration, as well as the photophysics predicted by solving the master equation of PDDEM using the FT (*dashed line*). The data refer to the case U2I for which the configuration Ω = (45°, 28°, 29°) and the rotational correlation times and fluorescence lifetimes are related as $\phi_\alpha = \phi_\beta = \tau_{\alpha 1} = \tau_{\beta 1}$= 5 ns

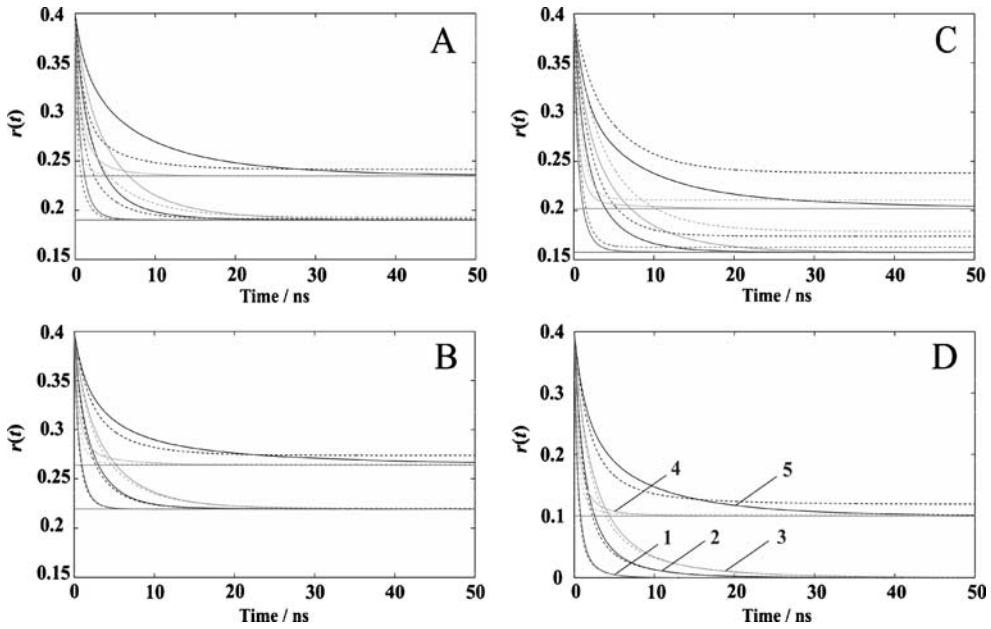

Fig. 3 The graphs compare the fluorescence anisotropy predicted by the EFT (*solid line*) and the FT (*dashed line*) for different configurations, Ω. The numbers 1-5 refer to the five cases defined in Table 1. The order of the graphs in the panels is the same as that shown in panel D. **A**: The configuration $\Omega = (45^o, 58^o, 29^o)$ and the dynamics refer to five cases, *i.e.* U1I-U5I. The calculated plateau values $r(t_\infty) = 0.190$ and 0.262 refer to two reorienting donors and one reorienting donor, respectively. **B**: The configuration $\Omega = (40^o, 40^o, 11^o)$ and the dynamics refer to five cases, *i.e.* U1II -U5II. The calculated plateau values $r(t_\infty) = 0.220$ and 0.301 refer to two reorienting donors and one reorienting donor, respectively. **C**: The configuration $\Omega = (41^o, 12^o, 71^o)$ and the dynamics refer to five cases, *i.e.* U1III - U5III. The calculated plateau values $r(t_\infty) = 0.158$ and 0.262 refer to two reorienting donors and one reorienting donor, respectively. For **A-C** a cone width of $\beta_c = 35°$ was used in the EFT. **D**: The two interacting donor groups are isotropically oriented. The calculated plateau values $r(t_\infty) = 0$ and 0.100 refer to two reorienting donors and one reorienting donor, respectively

whereas for systems in which one of the donor groups is immobilised the corresponding level is

$$r(t_\infty) = r_0 \left\{ \begin{array}{c} 1 + \left\langle D_{00}^{(2)}(\beta_{M_j D_j}) \right\rangle^2 + \left\langle D_{00}^{(2)}(\beta_{M_\alpha D_\alpha}) \right\rangle \\ \left\langle D_{00}^{(2)}(\beta_{M_\beta D_\beta}) \right\rangle D_{00}^{(2)}(\delta) \end{array} \right\} \quad (11)$$

From Eqs. 10–11 combined with the defined range of values of the order parameter ($0 \le \left\langle D_{00}^{(2)}(\beta_{M_j D_j}) \right\rangle^2 \le 1$), it follows that the stationary levels of the residual anisotropies are always higher for the system with an immobilised donor. This statement is exemplified by the results shown in Fig. 3. The plateau values of the anisotropy predicted by the EFT for two interacting and reorienting donor groups are in perfect agreement with independently calculated values. Note that the residual levels are exactly those obtained for a true DDEM, *i.e.* between donors exhibiting the same single exponential decay of the fluorescence. Thus the influence of PDDEM is not contributing to the $r(t_\infty)$value, as is the case for a true PDDEM system[13]. This conclusion has interesting consequences, which are discussed in the next section. The anisotropy plateau predicted by the FT only occasionally agrees with the level calculated from Eqs. 10–11, as could be seen from Fig. 3. Provided the coupling strengths in the FT are increased sufficiently, however, the levels do coincide with the expected values. This means that an analysis by the FT would in general underestimate the true distance between the donors. Except for the initial part of the $r_{FT}(t)$, the time dependence substantially deviates from that predicted by the EFT.

Joint studies of DDEM and PDDEM

Fluorescent probes linked to macromolecules rarely show single exponential decays. For instance, the fluorescence decay from BODIPY-labelled proteins usually exhibits a small and experimentally significant fraction of a second lifetime component. Often this component is similar irrespective of the labelling position. Therefore a careful data analysis of the energy transport is preferably based on combining the EFT of DDEM and PDDEM, as discussed above. In such an analysis the involved parameters are the donor-donor distance and the three configuration angles. For the determination of these parameters, additional experimental data regarding the system would facilitate the analyses. A feasible approach would be to study the perturbation of the time-resolved fluorescence lifetime and depolarisation in the presence of quenchers, which would unequally quench the two labelled positions, *e.g.* in a

protein molecule. Then, the observation of different donor decay rates is compatible with a true PDDEM system. Previously it was found that in PDDEM systems[13], the values of the residual anisotropy differ from those predicted by Eqs. 10–11. Unfortunately, no explicit relation exists between $r(t_\infty)$ and the EFT of PDDEM. This is a drawback, considering the fact that $r(t_\infty)$ reports on the value of $D_{00}^{(2)}(\delta)$. However, this value can be determined from the DDEM experiments, as well as from studies of the combined DDEM and PDDEM systems, which have been discussed in the present work. Actually, knowledge of δ, *i.e.* the angle between the symmetry axis of the potentials[11], introduces restrictions on the configuration space. Taken together, the joint PDDEM and DDEM experiments analysed by means of EFT would increase the stability of the data analyses.

Concluding remarks

The apparent DDEM, or homotransfer, within photophysically and chemically identical donor groups has been studied. For this, the most elaborate theory of energy transfer available has been used to predict experimental data, which are relevant for bifluorophoric systems with local order and reorientation dynamics. The data have been compared with those expected from the classical theory of Förster. While the relative fluorescence quantum yields usually agree within experimental accuracy, the steady-state and, in particular the time-resolved depolarisation data are considerably different.

Acknowledgements This work was financially supported by the Swedish Research Council and the Kempe Foundations.

References

1. Stryer L, Haugland RP (1967) Energy Transfer: A Spectroscopic Ruler. Proc. Natl. Acad. Sci. USA 58:719–726. doi:10.1073/pnas.58.2.719
2. Van der Meer BW, Coker G, III, Chen S-YS (1994) Resonance Energy Transfer: Theory and Data. VCH Publishers, Inc.
3. Kalinin S, Johansson LB-Å (2004) Utility and Considerations of Donor-Donor Energy Migration as a Fluorescence Method for Exploring Protein Structure-Function. J. Fluorescence 14:681–691. doi:10.1023/B:JOFL.0000047218.51768.59
4. Lakowicz JR (2006) Principles of Fluorescence Spectroscopy. Springer, Singapore
5. Förster T (1948) Zwischenmolekulare Energiewanderung und Fluorescenz. Ann. Phys. 2:55–75. doi:10.1002/andp.19484370105
6. Dale RE, Eisinger J, Blumberg WE (1979) The Orientational Freedom of Molecular Probes. The Orientation Factor in Intramolecular Energy Transfer. Biophys. J. 26:161–194. doi:10.1016/S0006-3495(79)85243-1
7. Haas E, Katchalski-Katzir E, Steinberg IZ (1978) Effect of the Orientation of Donor and Acceptor on the Probability of Energy Transfer Involving Electronic Transitions of Mixed Polarization. Biochemistry 17:5064–5070. doi:10.1021/bi00616a032
8. Johansson LB-Å, Bergström F, Edman P, Grechishnikova IV, Molotkovsky JG (1996) Electronic Energy Migration and Molecular Rotation within Bichromophoric Macromolecules. Part 1. Test of a Model using bis(9-anthrylmethylphosphonate) bisteroid. J. Chem. Soc., Faraday Trans. 92:1563–1567. doi:10.1039/ft9969201563
9. Steinberg IZ (1971) Long-Range Nonradiative Transfer of Electronic Excitation Energy in Proteins and Polypeptides. Annu. Rev. Biochem. 40:83–114. doi:10.1146/annurev.bi.40.070171.000503
10. Johansson LB-Å, Edman P, Westlund P-O (1996) Energy migration and rotational motion within bichromophoric molecules. II. A derivation of the fluorescence anisotropy. J. Chem. Phys. 105:10896–10904. doi:10.1063/1.472859
11. Isaksson M, Hägglöf P, Håkansson P, Ny T, Johansson LB-Å (2007) Extended Förster Theory for Determining Intraprotein Distances: 2. An Accurate Analysis of Fluorescence Depolarisation Experiments. Phys. Chem. Chem. Phys. 9:3914–3922. doi:10.1039/b701591g
12. Isaksson M, Norlin N, Westlund P-O, Johansson LB-Å (2007) On the Quantitative Molecular Analysis of Electronic Energy Transfer within Donor-Acceptor Pairs. Phys. Chem. Chem. Phys. 9:1941–1951. doi:10.1039/b614817d
13. Norlin N, Håkansson P, Westlund P-O, Johansson LB-Å (2008) Extended Förster Theory of Partial Donor-Donor Energy Migration (PDDEM): The κ^2-Dynamics and Fluorophore Reorientation. Phys. Chem. Chem. Phys. 10:6962–6970. doi:10.1039/b810661d
14. Engelborghs Y (2001) The analysis of time resolved protein fluorescence in multi-tryptophan proteins. Spectrochim. Acta A Mol. Biomol. Spectrosc. 57:2255–2270. doi:10.1016/S1386-1425(01)00485-1
15. Engelborghs, Y.: Correlating protein structure and protein fluorescence. J. Fluoresc. **13**, 9–16 (2003) doi:10.1023/A:1022398329107
16. Isaksson M, Kalinin S, Lobov S, Wang S, Ny T, Johansson LB-Å (2004) Distance Measurements in Proteins by Fluorescence Using Partial Donor-Donor Energy Migration (PDDEM). Phys. Chem. Chem. Phys. 6:3001–3008. doi:10.1039/b403264k
17. Kalinin SV, Molotkovsky JG, Johansson LB-Å (2002) Partial Donor-Donor Energy Migration (PDDEM) as a Fluorescence Spectroscopic Tool of Measuring Distances in Biomacromolecules. Spectrochim. Acta A Mol. Biomol. Spectrosc. 58:1087–1097. doi:10.1016/S1386-1425(01)00613-8
18. Kubo, R., Toda, M., Hashitsme, N.: (1985) Statitistical Physics II: Nonequilibrium Statistical Mechanics, Heidelberg
19. Fedchenia II, Westlund P-O, Cegrell U (1993) Brownian dynamic simulation of restricted molecular diffusion the symmetric and deformed cone model. Mol. Simul. 11:373–393. doi:10.1080/08927029308022521
20. Edman P, Håkansson P, Westlund P-O, Johansson LB-Å (2000) Extended Förster Theory of Donor-Donor Energy Migration in Bifluorophoric Macromolecules. Part I. A New Approach to Quantitative Analyses of the Time-Resolved Fluorescence Anisotropy. Mol. Phys. 98:1529–1537. doi:10.1080/002689700419752
21. Edman P, Westlund P-O, Johansson LB-Å (2000) On determining intramolecular distances from donor-donor energy migration (DDEM) within bifluorophoric macromolecules. Phys. Chem. Chem. Phys. 2:1789–1794. doi:10.1039/a909701e
22. Valeur, B.: (2002) Molecular Fluorescence. Principles and Applications. Wiley-VCH
23. Jablonski A (1950) Influence of torosional vibrations of luminescent molecules on the fundamental polarisation of photoluminiscence of solutions. Acta Physiol. Pol. 10:33–36
24. Brink DM, Satchler GR (1993) Angular Momentum. Clarendon Press, Oxford